Cytoskeleton Confinement and Tension of Red Blood Cell Membranes

N. Gov, A. G. Zilman, and S. Safran

Department of Materials and Interfaces, The Weizmann Institute of Science, P.O.B. 26, Rehovot, Israel 76100

(Received 22 July 2002; published 4 June 2003)

We analyze theoretically both the static and dynamic fluctuation spectra of the red blood cell in a unified manner, using a simple model of the composite membrane. In this model, the two-dimensional spectrin network that forms the cytoskeleton is treated as a rigid shell, located at a fixed, average distance from the lipid bilayer. The cytoskeleton thereby confines both the static and dynamic fluctuations of the lipid bilayer. The sparse connections of the cytoskeleton and bilayer induce a surface tension, for wavelengths larger than the bilayer persistence length. The predictions of the model give a consistent account for both the wave vector and frequency dependence of the experimental data.

DOI: 10.1103/PhysRevLett.90.228101 PACS numbers: 87.68.+z, 83.60.–a, 87.16.–b, 87.17.–d

A long-standing problem in the study of red blood cell (RBC) structure is the simultaneous softness of its membrane observed by thermal fluctuations [1] and the strong shear elasticity found in static deformation experiments, such as micropipette aspiration [2] and electrodeformation [3]. The membrane itself is a composite structure [4] with an outer, gel-like extracellular network of long sugar molecules (thought to be irrelevant to the structural strength), a mixed lipid/protein fluid bilayer and an attached, intracellular network. Previous theoretical models of this membrane treated it as a single, polymerized network with the combined curvature bending modulus of the lipid bilayer κ and the shear rigidity of the cytoskeleton μ [5]. Such models were successful in describing the response of the membrane in static *deformation* experiments, which give $\mu \sim 10^{-5}$–10^{-6} J/m^2 [2,3,6]. However, comparing these models to the *fluctuation* data leads to the conclusion that the membrane behaves as if the shear modulus vanishes $\mu \sim 0$ [5,7]. This surprising conclusion comes from the shape and amplitude analysis of the longest wavelength shape fluctuations [1,8].

The previous studies were concerned with the shape fluctuations of longest wavelength (of the order of the size of the RBC) [1,8]. Here, we focus on the fluctuation spectrum, at length scales of $1 - 0.1$ μm, where the effect of the cytoskeleton is clearly observed [9]. The important question is to what extent the cytoskeleton effects are distinguishable from the fluctuations of a free, closed bilayer. Our main result is that for a consistent description of both the static and the dynamic fluctuation spectrum we *must* include the confining effects of the cytoskeleton, whose sparse connections to the membrane result in a large effective surface tension. As in previous analysis of the experiments [1–9], the RBC fluctuations are treated in terms of thermodynamic equilibrium. We assume that the active processes are uncorrelated at the length scales of interest, and their main effect is to increase the effective temperature of the membrane [10].

The RBC cytoskeleton is a two-dimensional, roughly triangular, network of spectrin proteins [11] that is attached to the lipid bilayer at the nodes and at additional, random sites along the spectrin polymers. The cytoskeleton is well described as a network of entropic springs, of length $l \sim 80$ nm [11,12], with an effective spring constant: $\sim 4 \times 10^{-6}$ J/m^2, which is close to the measured static shear modulus: $\mu \simeq 6 \times 10^{-6}$ J/m^2 [2]. Compared with the lipid bilayer bending modulus $\kappa \simeq 2 \times 10^{-20}$ J [13], the curvature bending modulus of the cytoskeleton is negligible [1,14]: $\kappa_{\text{cyto}} \sim \mu w^2 \sim 10^{-21}$–$10^{-22}$ J for a cytoskeleton thickness of $w \sim 10$–50 nm.

We now begin by analyzing the measured static correlations [9] at the length scales of $1 - 0.1$ μm, and describe the effects of the cytoskeleton on the bilayer in terms of continuum mechanics. This is feasible since the cytoskeleton forms a rather open mesh that is attached to the bilayer at discrete points with a contact area that is small (~ 1 nm) compared to the internode distance (~ 100 nm). In a coarse-grained picture, we describe the thermal fluctuations of the bilayer with a continuum free energy functional

$$F \simeq \int dS \left[\frac{1}{2} \sigma (\nabla h)^2 + \frac{1}{2} \kappa (\nabla^2 h)^2 + \frac{1}{2} \gamma h^2 \right] \qquad (1)$$

that includes the usual bending energy of the bilayer (see, for example, [15]) in terms of the normal displacement h.

The inhomogeneous attachment of the cytoskeleton to the bilayer induces an effective surface tension σ and an overall confinement, modeled as a harmonic potential, characterized by γ. Both are related to the stiffness of the spectrin filaments that make up the cytoskeleton, as follows: The attachment of the cytoskeleton to the bilayer causes stretching and deformation of the bilayer [16], partly due to steric repulsion between the spectrin and the bilayer around the point of attachment [17]. Balancing the energies of the spectrin stretching and the local curvature of the bilayer predicts that the membrane has undulations of wavelength [16,18] $L \sim \sqrt{\kappa/\mu} \sim$ 100–200 nm and amplitude ~ 10 nm ($\sim w$) [1,14]. In our confining-shell model (1) this length scale is related

to the persistence length of the bilayer $\xi_0 = (\kappa/\gamma)^{1/4} \sim L$ [15], i.e., the wavelength above which the bilayer fluctuations are confined. In other words, we predict that the confinement potential is related to the spectrin stiffness by $\gamma \sim \mu/\xi_0^2 \sim 10^8$ J/m^4.

The last term in (1) is mathematically equivalent to a Lagrange multiplier that constrains the mean square amplitude of bilayer fluctuations to be equal to $d^2 = k_BT/8(\gamma\kappa)^{1/2}$ for an infinite bilayer. This term describes the effect of the cytoskeleton on the bilayer through a harmonic potential that maintains an average separation d (of order w) between the lipid bilayer and the cytoskeleton [15], here treated as an infinitely rigid shell that is separated from the bilayer. The discrete contacts that maintain the constant average separation are not specifically described in this continuum model; in a coarse-grained picture, these contacts are the physical origin of the constraint (potential) that determines the average membrane-spectrin network separation.

The surface tension coefficient that we expect from the constraining effect of the cytoskeleton-bilayer attachment is $\sigma \simeq \kappa/\xi_0^2$. This expression gives the effect of the bilayer shape constraint due to the cytoskeleton-induced deformations of lateral size ξ_0, described above. It turns out that this large cytoskeleton-induced surface tension is required to fit the experimental data, and is 2 orders of magnitude larger than the bare value that is due to surface area conservation: $\sigma_0 \sim \kappa/R^2 \sim 1 \times 10^{-9}$ J/m^2 (taking $R \sim 4$ μm as the RBC radius). At length scales shorter than ξ_0, we expect no stretching of the cytoskeleton, and the observed surface tension should approach the value of σ_0.

We now calculate the spatial correlations for a two-dimensional, flat bilayer, since for all but the largest wavelengths λ, the surface of the RBC is relatively flat: 50 nm $< \lambda <$ 1 μm $< R \sim 4$ μm. From Eq. (1) the equal-time (static) correlations of the normal deflections of the bilayer can be written [8,15]

$$\langle h_q h_{-q} \rangle = \frac{k_BT}{\kappa_q q^4}, \qquad \kappa_q = \kappa + \sigma q^{-2} + \gamma q^{-4}. \quad (2)$$

In the inset of Fig. 1 we plot the measured value of κ_q [9] in the form $(\kappa_q/\kappa - 1)^{-1}$ as a function of the normalized wave vector $(qd)^4$ [where $d^2 = k_BT/8(\gamma\kappa)^{1/2}$]. From the linear slope in the limit of $q \to 0$ we find the values of the confinement parameter $\gamma = 7.5 \times 10^7$ J/m^4 and $\gamma = 1.0 \times 10^7$ J/m^4 for the two cells measured. These values correspond to mean amplitudes $d \simeq 20$ and 35 nm and $\xi_0 = (\kappa/\gamma)^{1/4} = 130$ and 220 nm, respectively. At larger values of q there is a noticeable deviation from a straight line, arising from the effective surface tension $\sigma \sim 7.7 \times 10^{-7}$ J/m^2 and $\sigma \sim 2.8 \times 10^{-7}$ J/m^2 for the two cells. There is a rather abrupt change at the crossover wave vector $q_0 = 1/\xi_0$ (indicated by the vertical dotted lines in Fig. 1), above which surface tension approaches the bare value $\sigma \simeq \sigma_0 \sim 1.4 \times 10^{-9}$ J/m^2 (solid lines in Fig. 1).

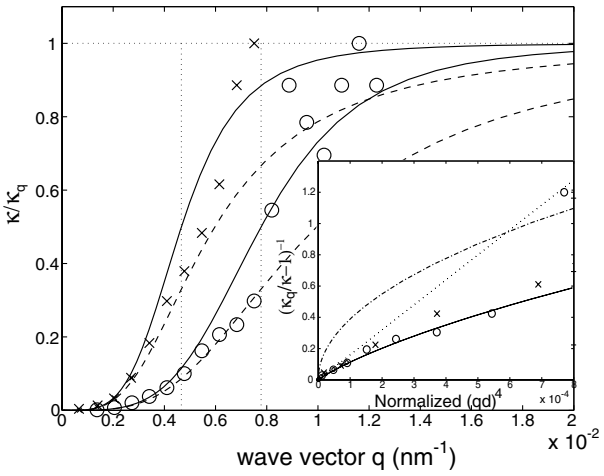

FIG. 1. The calculated [Eq. (2)] wave vector dependence of the bending modulus κ/κ_q of the RBC (solid lines: σ; dashed lines: σ_0) compared with the experimental data for the RBC [9] ($\bigcirc$, $\times$). The crossover wave vector q_0 is indicated by the vertical dotted lines. Inset: A plot of $(\kappa_q/\kappa - 1)^{-1}$ as a function of the normalized wave vector $(qd)^4$ for small wave vectors. The linear slope in the limit of $q \to 0$ is indicated by the dotted line. The deviation from linear behavior is well described by an effective surface tension $\sigma \simeq \kappa/\xi_0^2 \sim 2.8 \times 10^{-7}$ J/m^2 and 7.7×10^{-7} J/m^2 for the two cells (solid line). Note that surface tension alone ($\gamma = 0$), without the effect of the confining wall, does not describe the data (dash-dotted line).

The spread in the measured parameters could be related to differing experimental conditions and natural variations in the cytoskeleton network of RBC's. Note that surface tension alone, without the confining effect of the cytoskeleton (i.e., $\gamma = 0$), does not fit the data (dash-dotted line, Fig. 1 inset).

There is a qualitative difference in the power law of the wave vector dependence of κ_q for RBC and an empty lipid vesicle [19]. The vesicle is well described (Fig. 2) by Eqs. (1) and (2) with $\gamma = 0$, and an effective bare surface tension: $\sigma_0 \simeq \kappa_v/R_v^2 \sim 2 \times 10^{-10}$ J/m^2, where $R_v \sim 27$ μm and $\kappa_v \sim 1.3 \times 10^{-19}$ J are the vesicle radius and bending modulus, respectively. For the vesicle data, the rms thermal amplitudes are $d \simeq$ 1–1.5 μm (note that here d is not related to confinement). The data for the two RBC collapse on a single curve when the wavelength is scaled by the rms amplitude d (Fig. 2). The good scaling of the data indicates that there is indeed a single important length scale in the problem, namely, the persistence length ξ_0, that is in turn related to the cytoskeleton stiffness μ. This then determines the parameters appearing in the free energy, γ and σ, which are both crucial for fitting the data.

We now use the same simple model of spectrin confinement of the bilayer to describe the temporal correlations of the membrane fluctuations. The shape fluctuations of the RBC membrane are driven by both thermal and metabolic energies. The fluctuations which are dominated

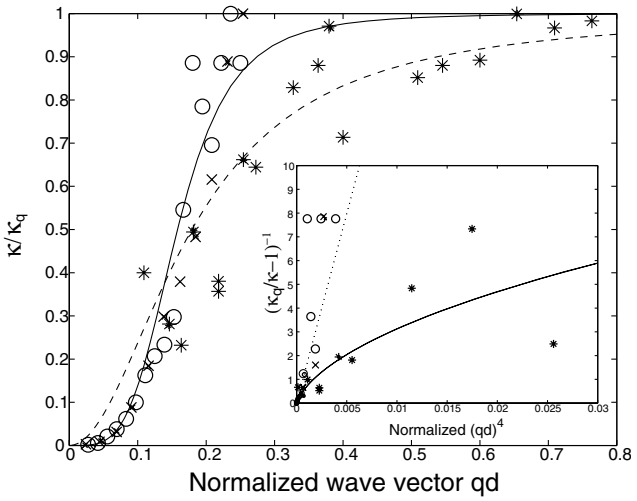

FIG. 2. A plot of the measured effective modulus κ/κ_q of the two RBC [9] (○, ×) and an empty giant vesicle [19] (*) as a function of the normalized wave vector qd. The graph shows the data collapse of the two RBC when the wave vector is normalized by the "wall" separation d. The calculations for the two RBC and the vesicle are given by the solid and dashed lines, respectively. Inset: A plot of $(\kappa_q/\kappa - 1)^{-1}$ as a function of the normalized wave vector $(qd)^4$ for small wave vectors. The linear slope in the limit of $q \to 0$ for the RBC is indicated by the dotted line. The calculation for the vesicle is given by the solid line.

by active processes have a frequency spectrum that is confined to the range 0.3–1 Hz [20]. We therefore limit our analysis to higher frequencies, for which it has been shown [10,20,21] that the active processes can be accounted for by an increase in the effective temperature. The temporal height-height correlation function [7,22] for a flat bilayer at a distance $D \sim d$ from a rigid wall, is

$$\langle h_q(t) h_{-q}(0)\rangle = \frac{k_B T}{\kappa_q q^4} e^{-\omega(q)t}, \tag{3}$$

where κ_q is given in (2). Using standard hydrodynamic techniques [22,23], we calculate [24] the hydrodynamic interaction $\Lambda(q)$ (Oseen interaction kernel)

$$\Lambda(q) = \Lambda_f(q) \times -e^{-2Dq}[1 - e^{2Dq} + 2Dq + 2(Dq)^2] \tag{4}$$

and the relaxation frequency $\omega(q) = [(\kappa q^4 + \sigma q^2 + \gamma)]\Lambda(q)$ for a membrane bounded by an impermeable wall [10,23] [$\Lambda_f(q) = 1/4\eta q$ for a free bilayer], where $\eta \sim 3\eta_{\text{water}}$ is some average viscosity of the cytoplasm and external solution [7]. In the limit of short wavelengths ($q \to \infty$) we recover the free bilayer frequency: $\omega(q) \to \kappa q^3/4\eta$. For intermediate wavelengths $q_0 \ll q \ll 1/D$, we recover the result of Brochard *et al.* [7]: $\omega(q) \to \kappa q^6 D^3/3\eta$. This is the range of wave vectors which is dominant for the RBC membrane fluctuations.

The mean square amplitude of the normal fluctuations, as a function of frequency ω, is the Fourier transform

$$d^2(\omega) = \frac{1}{(2\pi)^2}\int q dq \int \langle h_q(t) h_{-q}(0)\rangle e^{-i\omega t} dt = \frac{1}{(2\pi)^2}\int \frac{k_B T}{\kappa_q q^4}\frac{\omega(q)}{\omega(q)^2 + \omega^2} q dq. \tag{5}$$

For a free bilayer this expression (5) gives an anomalous frequency dependence [22]: $d^2(\omega) \propto \omega^{-5/3}$. We integrate the expression (5) numerically in the range $\pi/R < q < \pi/a$ ($a \simeq 5$ nm), and compare with the experimental data [20]. In the inset of Fig. 3 we plot $d(\omega)$ using the parameters of the two cells of Fig. 1, and the larger value of the effective surface tension, since we are in the range $q \lesssim q_0$, and the membrane feels the pull of the cytoskeletal contacts. The good agreement of both the static and dynamic data with our model, using similar values of the bilayer-spectrin spacing $D \simeq d$, shows the overall consistency of our confinement model. Additionally, we find that the spectrin mesh appears as an impermeable wall to bilayer fluctuations. This is because the rapid motion of the flexible spectrin filaments covers the holes in the mesh in a time [25] $\tau_r \sim \eta l^2/k_B T \sim 2\ \mu$sec, which is much shorter than the typical time of the bilayer fluctuations.

In the range $q_0 \ll q \ll 1/D$, we recover the earlier results [7,23] $d(\omega)^2 \propto \omega^{-4/3}$ (Fig. 3 inset). Note that in the work of Brochard *et al.* [7] the confinement is due to the finite thickness of the cell adhered to a substrate, not of the cytoskeleton. Our calculation has the advantage of consistently describing both the static (spatial) and

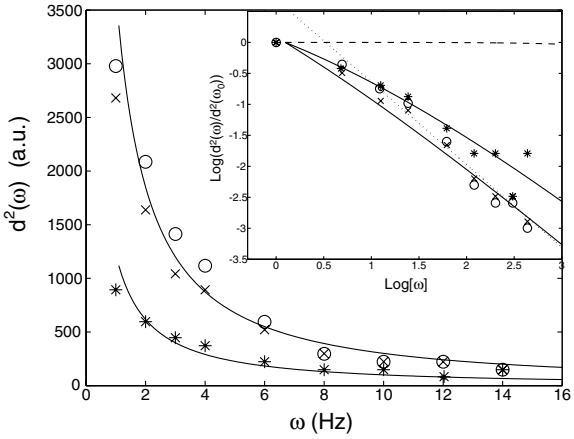

FIG. 3. Frequency dependence of the mean-square amplitude [20] $d^2(\omega)$ of the RBC (○), showing the reduction in the amplitude due to partial ATP depletion (×) and complete absence (RBC ghost) (*). The lines are fits to Eq. (5). The ATP depleted system shows only thermal fluctuations, while the normal RBC shows fluctuations whose amplitude is enhanced by a factor of ~3 (solid lines). We use the parameters of the soft RBC of Figs. 1 and 2. Inset: A normalized log-log plot showing the power law dependence ($\omega_0 = 1$ Hz). The two sets of calculations are for both RBC's of Fig. 1 (solid lines). The dotted line shows the regime where $d^2(\omega) \propto \omega^{-4/3}$. The case of a free bilayer, without the hydrodynamic effect of the rigid wall, is in complete disagreement with the data (dashed line).

dynamic (temporal) fluctuation data. Note that the case of a pure bilayer with large effective surface tension σ, but without the hydrodynamic effect of the rigid wall, is in complete disagreement with the data (dashed line, Fig. 3 inset). The thin water layer trapped between the bilayer and the spectrin mesh is isolated from the flows of the cytoplasm.

In Fig. 3 we show that the fluctuation amplitude of normal RBC, adenosine triphosphate(ATP)-depleted RBC, and RBC ghost, are all described by the same expression (5) (using in our calculation the values of γ and σ for the softer cell [26] of Fig. 1), differing only by an enhancement factor of ~ 3, due to the effective temperature of active processes [21].

While this model accounts for the wave vector dependence of the statics and the frequency dependence of the dynamics, the absolute amplitude of the fluctuations and the different values observed in active and ATP-depleted cells must still be explained. One possibility is that ATP-driven structural rearrangement in the spectrin network [1,4,6] determines the amplitude of the largest wavelength (and lowest frequency) fluctuations [20]. These ATP-driven conformational changes can give rise to local defects in the triangular spectrin network, resulting in nodes with more or less than six spectrin bonds. The local curvature of the cytoskeleton may change at the site of a defect, from being locally flat (six bonds) to having a ~ 80 nm deviation out of the plane of the flat cytoskeleton (fivefold node). The effect of this random (uncorrelated) buckling is to increase the mean bilayer-rigid shell separation by a factor of ~ 4. According to our model, this will increase the amplitude of the $q \rightarrow 0$ modes by a factor of $\sim 4^4$, as measured [5]. At shorter wavelengths the fluctuations can be treated as in thermodynamic equilibrium, with a higher effective temperature, as discussed above. We indeed showed that both the statics and dynamics of these fluctuations can be described with a unified model.

We thank R. Korenstein, E. Sackmann, and H. Strey for useful discussions. This work was supported by the ISF grant. The authors are grateful to the donors of the Petroleum Research Fund administered by the American Chemical Society and to the Schmidt Minerva Center for their support. N. G.'s research is supported by the Koshland Foundation.

[1] H. Strey, M. Peterson, and E. Sackmann, Biophys. J. **69**, 478 (1995).
[2] D. Discher, N. Mohandas, and E. A. Evans, Science **266**, 1032 (1994); V. Heinrich, K. Ritchie, N. Mohandas, and E. Evans, Biophys. J. **81**, 1452 (2001).
[3] H. Engelhardt, H. Gaub, and E. Sackmann, Nature (London) **307**, 378 (1984).
[4] E. Sackmann, FEBS Lett. **346**, 3 (1994).
[5] M. A. Peterson, Phys. Rev. A **45**, 4116 (1992).
[6] J. C-M. Lee and D. E. Discher, Biophys. J. **81**, 3178 (2001).
[7] F. Brochard and J. F. Lennon, J. Phys. (Paris) **36**, 1035 (1975).
[8] M. Peterson, H. Strey, and E. Sackmann, J. Phys. II (France) **2**, 1273 (1992).
[9] A. Zilker, H. Engelhardt, and E. Sackmann, J. Phys. (Paris) **48**, 2139 (1987).
[10] J. Prost, J.-B. Manneville, and R. Bruinsma, Eur. Phys. J. B **1**, 465 (1998).
[11] V. Bennett, Biochim. Biophys. Acta **988**, 107 (1989).
[12] E. Sackmann, in *Structure and Dynamics of Membranes*, edited by R. Lipowsky and E. Sackmann (Elsevier, Amsterdam, 1995), Vol. 1A, p. 1.
[13] For the curvature bending modulus κ of the lipid bilayer [U. Seifert and R. Lipowsky, in *Structure and Dynamics of Membranes* (Ref. [12]), p. 403]. We use the smallest value which is deduced from the amplitude of thermal fluctuations at the smallest measured wavelengths [9] $\kappa \simeq 2 \pm 1 \times 10^{-20}$ J.
[14] L. D. Landau and E. M. Lifshitz, *Theory of Elasticity* (Pergamon Press, New York, 1981); A. H. Swihart, J. M. Mikrut, J. B. Ketterson, and R. C. Macdonald, J. Microscopy **204**, 212 (2001); S. K. Boey, D. H. Boal, and D. E. Discher, Biophys. J. **75**, 1573 (1998).
[15] S. A. Safran, *Statistical Thermodynamics of Surfaces, Interfaces and Membranes*, Frontiers in Physics Vol. 90 (Addison-Wesley Publishing Company, Reading, MA, 1994).
[16] K. Zeman, H. Engelhardt, and E. Sackmann, Eur. Biophys. J. **18**, 203 (1990).
[17] M. Breidenich, R. R. Netz, and R. Lipowsky, Europhys. Lett. **49**, 431 (2000); R. Lipowsky, H-G. Dobereiner, C. Hiergeist, and V. Indrani, Physica A (Amsterdam) **249**, 536 (1998).
[18] Another way to derive the amplitude of the spontaneous bilayer undulations is to compare the steric repulsion of the bilayer thermal fluctuations per area with the area modulus of the cytoskeleton: $\mu \simeq (k_B T)^2/\kappa d^2 \Rightarrow d \sim 10$ nm $\sim w$ [see J. O. Radler, T. J. Feder, H. H. Strey, and E. Sackmann, Phys. Rev. E **51**, 4526 (1995)].
[19] W. Hackl, U. Seifert, and E. Sackmann, J. Phys. II (France) **7**, 1141 (1997).
[20] S. Tuvia, S. Levin, A. Bitler, and R. Korenstein, J. Cell Biol. **141**, 1551 (1998); S. Levin and R. Korenstein, Biophys. J. **60**, 733 (1991).
[21] J.-B. Manneville, P. Bassereau, D. Levy, and J. Prost, Phys. Rev. Lett. **82**, 4356 (1999).
[22] A. G. Zilman and R. Granek, Phys. Rev. Lett. **77**, 4788 (1996).
[23] U. Seifert, Phys. Rev. E **49**, 3124 (1994).
[24] A. G. Zilman and N. Gov (to be published). We also calculated the hydrodynamic interactions for a permeable wall, but since the permeation length $L_p = \lambda\eta \lesssim 10^{-2}$ nm (where λ is the permeability of the spectrin mesh [10]) turns out to be $L_p q \ll 1$ for the RBC, we can regard the cytoskeletal shell as an impermeable wall.
[25] M. Doi, *Introduction to Polymer Physics* (Clarendon Press, Oxford, 1996).
[26] We use one of the two RBC arbitrarily; the fits would be just as good if we used the other RBC.